

# A collapse of the cross-spectral function in phase noise metrology

C. W. Nelson, A. Hati, and D. A. Howe

National Institute of Standards and Technology, 325 Broadway, Boulder, Colorado 80305, USA

(Received 11 September 2013; accepted 1 February 2014; published online 25 February 2014)

Cross-spectral analysis is a mathematical tool for extracting the power spectral density of a correlated signal from two time series in the presence of uncorrelated interfering signals. We demonstrate and explain a set of amplitude and phase conditions where the detection of the desired signal using cross-spectral analysis fails partially or entirely in the presence of a second uncorrelated signal. Not understanding when and how this effect occurs can lead to dramatic under-reporting of the desired signal. Theoretical, simulated and experimental demonstrations of this effect as well as mitigating methods are presented. [<http://dx.doi.org/10.1063/1.4865715>]

## I. INTRODUCTION

The detection of a signal in the presence of interfering noise always presents a challenge. The power spectral density (PSD) of an ergodic and stationary signal can be determined from the cross-spectrum even in the presence of interfering noise. If one can create two reproductions of a desired signal and the interfering noise in each copy is not correlated, the average of the cross-spectrum can be used to estimate the PSD of the desired signal even when the intensity of the interfering noise is dominant. Cross-spectral analysis has been used to improve the sensitivity of measurements in the field of modulation noise metrology for nearly fifty years.<sup>1–5</sup> The last twenty years have seen extensive use of cross-spectral analysis in the laboratory<sup>6–12</sup> and it has even made its way into commercial test equipment, at first with small companies<sup>8,13</sup> and now with major test equipment manufacturers. It is generally understood that when a desired signal has some level of correlation with an interferer, occasionally some level of cancellation of signals can be observed. We will demonstrate and explain a set of conditions where the detection of the desired signal using cross-spectral analysis collapses partially or entirely in the presence of a second uncorrelated interfering signal. This effect was first observed by Ivanov and Walls in 2000,<sup>14,15</sup> and in this paper we refine the previous discussion by proposing that the failure to correctly detect the measured noise occurs when a special phase condition exists between the signals being presented to the cross-spectrum function. Significantly, this paper's findings may negate many overly optimistic and untrue low-noise results of past measurements. Unfortunately, there is no easy way to determine whether a past cross-correlation measurement was affected by the cause given in this paper.

## II. THE CROSS-POWER SPECTRAL DENSITY

The cross-spectrum of two signals  $x(t)$  and  $y(t)$  is defined as the Fourier transform of the cross-covariance function of  $x$  and  $y$ . However, from the Wiener–Khinchin theorem, it can be implemented far more practically by the metrologist as

$$\begin{aligned} X(f) &= F\{x(t)\}, \\ Y(f) &= F\{y(t)\}, \\ \langle S_{xy}(f) \rangle_m &= \frac{1}{T} \langle X(f)Y^*(f) \rangle_m, \end{aligned} \quad (1)$$

where  $X(f)$  and  $Y(f)$  are the truncated Fourier transforms of  $x(t)$  and  $y(t)$  and  $\langle \rangle_m$  denotes an ensemble of  $m$  averages.  $T$  is the measurement or truncation time normalizing the PSD to 1 Hz and “\*” indicates complex conjugate. The cross-power spectral density  $S_{xy}(f)$  can thus be determined from the ensemble average of the product of  $X(f)$  and the complex conjugate of  $Y(f)$ . Unlike a normal PSD, the cross-PSD is a complex quantity. An excellent detailed description of the cross-spectrum and its estimators is available from Rubiola and Vernotte.<sup>16</sup> In this section, we highlight different scenarios of cross-spectrum analysis. Although two-sided Fourier transforms and spectra are typically preferred for theoretical discussions, we will be using single-sided representations exclusively in this paper.

**Case i:** Suppose we have two signals  $x(t)$  and  $y(t)$ , each composed of three statistically independent, ergodic, and random processes  $a(t)$ ,  $b(t)$ , and  $c(t)$  such that

$$\begin{aligned} x(t) &= a(t) + c(t), \\ y(t) &= b(t) + c(t), \end{aligned} \quad (2)$$

then we consider  $c(t)$  to be the desired signal that we wish to recover, and  $a(t)$  and  $b(t)$  are the uncorrelated interfering signals. The Fourier transforms of these signals are represented by the corresponding capitalized variables as

$$\begin{aligned} X(f) &= A(f) + C(f), \\ Y(f) &= B(f) + C(f), \end{aligned} \quad (3)$$

and the cross-PSD is represented by

$$\begin{aligned} \langle S_{xy}(f) \rangle &= \frac{1}{T} \langle X(f)Y^*(f) \rangle \\ &= \frac{1}{T} \langle (A+C)(B+C)^* \rangle \\ &= \frac{1}{T} \left[ \langle CC^* \rangle + \langle \cancel{CB^*} \rangle + \langle \cancel{AC^*} \rangle + \langle \cancel{AB^*} \rangle \right] \\ &= S_c(f). \end{aligned} \quad (4)$$

Equation (4) shows that the cross-terms average to zero, indicate by the  $X$ 's, and the expectation of the cross-spectrum gives the power spectral density,  $S_c(f)$  of the signal  $c(t)$ . In practice, when the cross-spectrum is calculated, the contributions of  $a(t)$  and  $b(t)$  are reduced by the square root of the observation time.

**Case ii:** If signal  $c(t)$  is presented to the cross-spectrum function in an anti-correlated or phase inverted sense as in Eq. (5), the magnitude of the averaged cross-spectrum still gives the same result. However, the phase angle of the complex quantity would average to  $\pi$ :

$$x(t) = a(t) + c(t), \quad (5)$$

$$y'(t) = b(t) - c(t),$$

$$|\langle S_{xy}(f) \rangle| = |\langle S_{xy'}(f) \rangle|. \quad (6)$$

**Case iii:** Now, we introduce a fourth random process,  $d(t)$ , another independent, ergodic variable as follows:

$$x(t) = a(t) + c(t) + d(t), \quad (7)$$

$$y(t) = b(t) + c(t) + d(t).$$

If  $d$  is also correlated in both  $x$  and  $y$ , then the cross-spectrum converges to the sum of the average spectral densities of  $c$  and  $d$ :

$$\langle S_{xy}(f) \rangle = S_c(f) + S_d(f). \quad (8)$$

The cross-power spectral density is unable to discern between the two correlated signals and converges to the combination of both. This commonly occurs when amplitude modulation (AM) noise from a source contaminates a phase modulation (PM) measurement via an imperfect mixer.<sup>17-19</sup>

**Case iv (collapse of the cross-spectral function):** However, if  $c(t)$  is correlated in  $x(t)$  and  $y(t)$  and  $d(t)$  is anti-correlated (phase inverted) in  $x$  and  $y$  an unexpected outcome occurs:

$$x(t) = a(t) + c(t) + d(t), \quad (9)$$

$$y(t) = b(t) + c(t) - d(t).$$

The corresponding Fourier transforms and the cross-PSD are represented by

$$X = A + C + D, \quad (10)$$

$$Y = B + C - D,$$

$$\begin{aligned} \langle S_{xy}(f) \rangle &= \frac{1}{T} \langle XY^* \rangle \\ &= \frac{1}{T} \langle (A+C+D)(B+A-D)^* \rangle \\ &= \frac{1}{T} \langle CC^* \rangle - \langle DD^* \rangle + \cancel{\langle AB^* \rangle} + \cancel{\langle AC^* \rangle} \\ &\quad - \cancel{\langle AD^* \rangle} + \cancel{\langle CB^* \rangle} - \cancel{\langle CD^* \rangle} + \cancel{\langle DB^* \rangle} + \cancel{\langle DC^* \rangle} \end{aligned} \quad (11)$$

$$\langle S_{xy}(f) \rangle = \frac{1}{T} [\langle CC^*(f) \rangle - \langle DD^*(f) \rangle]. \quad (12)$$

What (12) tells us is that at any frequency  $f$  where the average magnitude of signal  $C(f)$  is equal to that of signal  $D(f)$ , the cross-spectrum collapses to zero. Any contribution of the desired signal  $c(t)$ , or the interferer  $d(t)$ , to the cross spectral density is eliminated. This occurs even though signals  $c(t)$  and  $d(t)$  are completely uncorrelated. If the PSDs of the two signals are exactly equal, the amount of observed cancellation is limited to  $\sqrt{m}$ , where  $m$  is the number of averages. If  $C(f)$

and  $D(f)$  have the same shape or slope versus frequency, entire octaves or decades of spectrum can be suppressed and be grossly under-reported. If the PSD of  $C$  and  $D$  are not exactly equal, a partial cancellation still occurs. The maximum amount of suppression in the magnitude of the cross-spectrum relative to the non-phase inverted measurement (Case iii) approaches

$$\frac{S_c(f) + S_d(f)}{\text{abs}(S_c(f) - S_d(f))}, \quad (13)$$

at the rate of  $1/\sqrt{m}$ . If the two signals have different frequency-dependent noise slopes, a characteristic notch will be observed in the magnitude of the cross spectrum. A differential delay between the two signals presented to the cross-spectrum function will also create a similar notch located at the reciprocal of the delay time.

### III. SIMULATION RESULTS: CASE III AND CASE IV

Simulations of the collapse of the cross-spectral function were created in Mathworks Simulink with the block diagram shown in Fig. 1. The cross-spectrum is a complex quantity and the optimal estimator for extracting the PSD of the signal present at both  $x$  and  $y$  is the real part of the ensemble average,  $\Re\{\langle S_{xy}(f) \rangle_m\}$ . Unfortunately, at small  $m$ , before it converges, this estimator can become negative. The desire to plot the results in logarithmic format necessitates use of a positive valued estimator. Biased, positive valued estimators are available, several versions using modifications of the real component of  $S_{xy}$  or the magnitude of the ensemble average can be used.<sup>16</sup> The optimal positive estimator with the lowest bias is typically not available on commercial laboratory equipment and must be implemented with a custom analyzer. The cross-spectral collapse described in this paper occurs regardless of the choice of estimator used. For the following numerical and experimental sections we will use the biased magnitude estimator  $|\langle S_{xy}(f) \rangle_m|$ , as well as its pair  $\arg\{\langle S_{xy}(f) \rangle_m\}$  for describing the amplitude and phase relationships. Although the magnitude estimator has the slowest convergence due to a substantial initial bias and may not be optimal for accurate measurements, we justify its use in these examples with its ease of availability, the large number of averages used, and because the choice of estimator is irrelevant in the demonstration of the cross-spectral collapse.

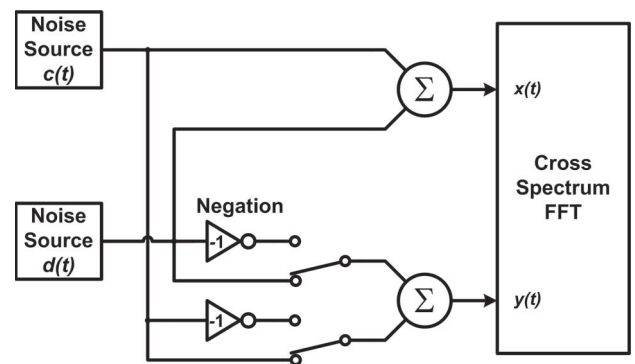


FIG. 1. Block diagram for a Mathworks Simulink simulation. A negation (gain = -1) is switch selectable for creating correlated and anti-correlated inputs to the cross-spectrum.

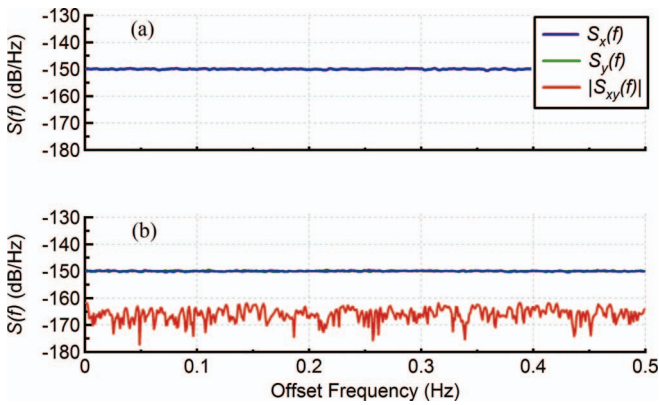


FIG. 2. Mathworks simulation results for the addition of two completely independent noise sources,  $c(t)$  and  $d(t)$ , each with power spectral density of  $-153$  dB/Hz relative to unity. The magnitude of the cross-spectrum for (a) occurs when  $x(t) = y(t) = c(t) + d(t)$  (Case iii) and all three traces coincide. The cross-spectrum for (b) occurs when  $x(t) = c(t) + d(t)$  and  $y(t) = c(t) - d(t)$  (Case iv). Both figures are for a 1024-point FFT and 1000 averages. The amount of cancellation is 15 dB and is proportional to the square root of the number of averages.

Two noise generators, which can create white or frequency-dependent noise slopes were summed and connected to both inputs of the cross-spectral density function. Two switches were provided to allow for the negation (gain =  $-1$ ) of either one or both signals to one input of the cross-spectrum. Placing only one or the other switch, but not both, into negation creates the collapse of the function (Fig. 2(b)). If none or both signals are negated, a normal cross-spectrum occurs (Fig. 2(a)). Finally, the collapse due to the interaction of two differently sloped noise types creates a notch shown in Fig. 3.

#### IV. CROSS-SPECTRUM PHASE NOISE MEASUREMENTS

A two-channel cross-spectrum phase-noise measurement system for measuring noise properties of an amplifier is shown in Fig. 4.<sup>5,16,17</sup> Each channel includes a phase shifter, a double-balanced mixer as a phase detector, and an inter-

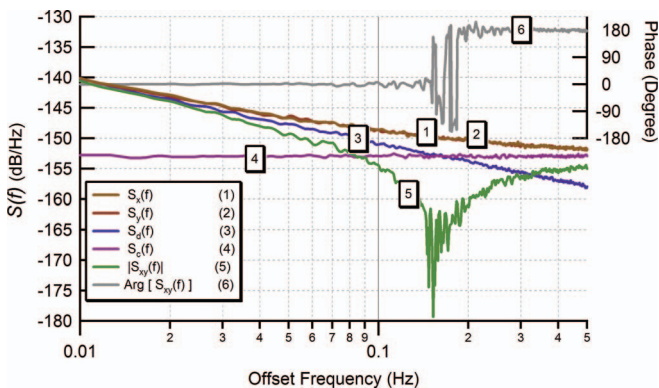


FIG. 3. Mathworks simulation results for the addition of two independent noise sources,  $c(t)$  and  $d(t)$ , with different frequency dependence. Signal  $S_c(f)$  has a power spectral density of  $-153$  dB/Hz relative to unity. Signal  $S_d(f)$  has a  $f^{-1}$  slope and intersects signal  $S_c(f)$  at a frequency of 0.164 Hz. The cross-spectrum is calculated with  $x(t) = c(t) + d(t)$ , and  $y(t) = c(t) - d(t)$  (Case iv). Both figures are for a 1024-point FFT and 1000 averages.

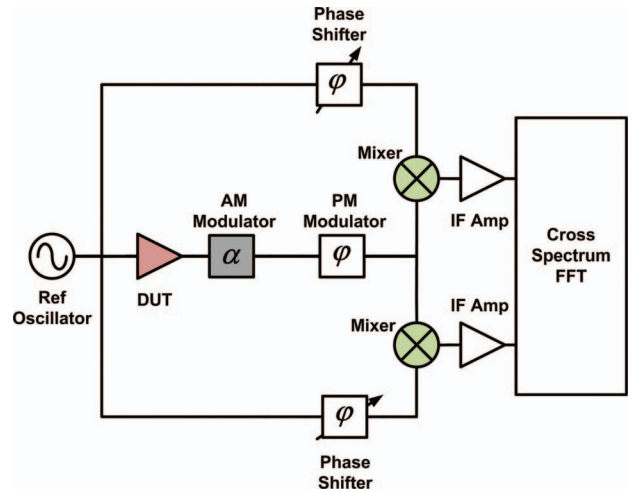


FIG. 4. Block diagram of a two-channel cross-spectrum system for measuring PM noise of an amplifier. DUT – Divider Under Test, IF AMP – Intermediate Frequency Amplifier, FFT – Fast Fourier Transform.

mediate frequency (IF) amplifier. The phase shifters establish phase quadrature between two signals at the mixer inputs. AM and PM modulators are also included for evaluating the sensitivities of the measurement system. The output of each mixer, after amplification, is analyzed with a two-channel cross-spectrum fast-Fourier-transform (FFT) spectrum analyzer. The voltage input signals to channel-1 and channel-2 of the FFT analyzer can be written, respectively, as

$$\begin{aligned} v_1(t) &= G_1[k_{d1}(\Phi_1)\varphi_{DUT}(t) + \beta_1(\Phi_1)\alpha(t) + v_{B1}(t)], \\ v_2(t) &= G_2[k_{d2}(\Phi_2)\varphi_{DUT}(t) + \beta_2(\Phi_2)\alpha(t) + v_{B2}(t)], \end{aligned} \quad (14)$$

where  $v_n(t)$  represents the voltage present at a given FFT channel number ( $n$ ),  $G_n$  is the gain of the baseband IF amplifier,  $k_{dn}$  is the voltage-to-phase conversion factor of the mixer,  $\varphi_{DUT}(t)$  represents the phase fluctuations of the device under test (DUT),  $\beta_n$  is the AM to voltage conversion factor of the mixer,  $\alpha(t)$  is the fractional amplitude fluctuations of the driving oscillator and the DUT, and  $v_{Bn}(t)$  is the combined baseband noise of the mixer and IF amplifier. The conversion factors ( $k_{dn}$ ,  $\beta_n$ ) for each mixer are highly dependent on the average phase shift ( $\Phi_n$ ) between its two inputs.

Fig. 5 shows the dependence of the conversion factors ( $k_d$ ,  $\beta$ ) on the phase shift between the input signals to an

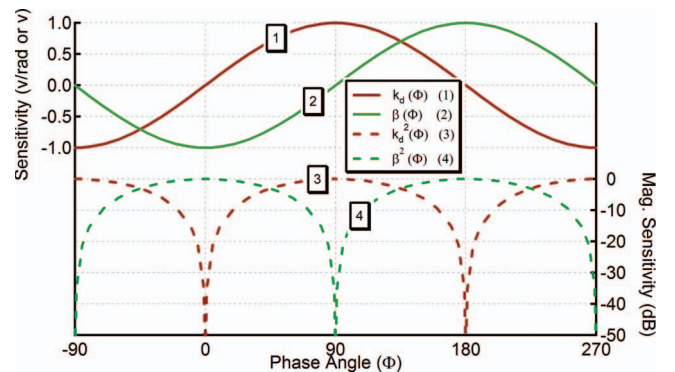


FIG. 5. Shows the dependence of the conversion factors ( $k_d$ ,  $\beta$ ) on average phase shift ( $\Phi$ ) for an ideal mixer operating linearly. The DC output voltage of the mixer will also follow the  $\beta(\Phi)$  curve.

TABLE I. Sign of conversions factors vs. mixer operating quadrant.

Quadrant	Range	Sign of $k_d$	Sign of $\beta$
<b>I</b>	$(0-\pi/2)$	+	-
<b>II</b>	$(\pi/2-\pi)$	+	+
<b>III</b>	$(\pi-3\pi/2)$	-	+
<b>IV</b>	$(3\pi/2-2\pi)$	-	-

ideal mixer. We can clearly see that the two sensitivities are orthogonal, and one or the other sensitivity is exclusive at the quadrant boundaries (Table I). Implementing a non-ideal mixer will typically distort the curves, introduce a phase offset, and disrupt the orthogonality of the two sensitivities. These aberrations from the ideal double-balanced mixer can be attributed to saturation and non-identically matched diodes and may be highly dependent on operating and environmental conditions. Operating a PM noise measurement with a high level of AM noise rejection can be challenging, and without careful tuning and control of the mixer phase shift,  $\Phi$ , the measurement system will typically show levels of AM rejection around 15–30 dB. One would like to operate the mixer in a PM noise measurement at what we call “true quadrature,” a phase shift usually near  $\pi/2$  or  $3\pi/2$ , where the sensitivity to AM ( $\beta$ ) goes through zero.<sup>18,19</sup> Finding this exact phase shift typically involves introduction of a sinusoidal AM modulation and tuning the phase shift to minimize the amount of AM leakage into the PM measurement. It is important to note that the sensitivity to AM and its minimum may be different for the RF and LO ports of a non-ideal mixer.<sup>19</sup>

Analyzing Eq. (14), we observe that  $\varphi_{DUT}(t)$  is correlated in both  $v_1(t)$  and  $v_2(t)$ , albeit via different conversion factors. The same is true for  $\alpha(t)$ , while the two baseband signals,  $v_{Bn}(t)$  are uncorrelated from each other. Furthermore, the two sets of conversion factors  $(k_{d1}, \beta_1)$  and  $(k_{d2}, \beta_2)$ , which dependent on their respective mixer phase shifts,  $\Phi_1$  and  $\Phi_2$ , can be set to 16 different quadrant combinations with varying correlation sense, half of which can create correlated/anti-correlated pairs as indicated in Table II.

When high levels of AM rejection are required and thus operating near the AM null, environmental and signal power changes may cause the location of the null or operating point to drift, causing the sign of  $\beta$  to flip. This may cause the noise cancellation effect to appear and disappear temporally, further masking its presence during an average. Measuring low lev-

TABLE II. Mixer quadrants pairs that may cause undesired cross-spectral cancellation. “OK” indicates that each conversion factor has the same sign of correlation in both mixers. “X” indicates a correlated and anti-correlated (Case iv) pair of conversion factors  $(k_d, \beta)$ .

Mixer 2 quadrant	Mixer 1 quadrant			
	<b>I</b>	<b>II</b>	<b>III</b>	<b>IV</b>
<b>I</b>	OK	X	OK	X
<b>II</b>	X	OK	X	OK
<b>III</b>	OK	X	OK	X
<b>IV</b>	X	OK	X	OK

els of PM noise in the presence of much higher AM levels requires continuous operation near the bottom of the null and may require pure AM modulators<sup>20,21</sup> and an active control servo to maintain a high level of AM suppression.

## V. EXPERIMENTAL RESULTS

In order to experimentally demonstrate the collapse of the cross-power spectral function, the setup described in Fig. 4 is used. An amplifier with high gain and low input power is used as the DUT to generate a signal with a high white PM noise level. The DUT has 42 dB of gain, and a noise figure of 7 dB, and is operating with an input power of  $-25$  dBm creating a single-sideband white PM noise level of  $\mathcal{L}(>10 \text{ kHz}) = -145$  dBc/Hz. Under these conditions, the noise of DUT dominates and the mixer’s residual noises are negligible. The PM noise of the DUT is shown as trace (4) in Fig. 6. An AM modulator is driven with white noise from a direct digital synthesizer (DDS), producing an AM level of  $-130$  dBc/Hz shown as trace (2). The phase shifters of both mixers are detuned from “true quadrature” so that the relative level of AM suppression ( $k_d/\beta$ ) of 15 dB is achieved. The amount of AM leakage into the PM noise measurement is measured and shown as trace (5). If we perform a cross-spectrum PM noise measurement with both mixers in the same quadrant (Case iii), we observe the expected result shown in trace (3). In this case the measured white PM noise is twice that of the DUT due to the presence of an equal amount of leakage white AM noise. If we now adjust the mixers to have the same amount of AM leakage, but place them in different quadrants (**I** and **II**) so that  $k_{d1} = k_{d2}$  and  $\beta_1 = -\beta_2$ , a correlated/anti-correlated pair of conversion factors are created (Case iv) and we now observe that the cross-spectrum approaches zero in the white region, as shown in trace (6). This annihilation occurs in the cross-spectrum even though the white PM noise of the amplifier and the leaked injected AM noise are entirely uncorrelated. The phase of the cross-spectrum, trace (1), shows that in the region where the cross-spectrum is still average-limited, the phase is random.

Another example is demonstrated in Fig. 7 where we reduced the amount of AM rejection in the mixer so that the level of leakage AM noise is slightly higher than the thermal

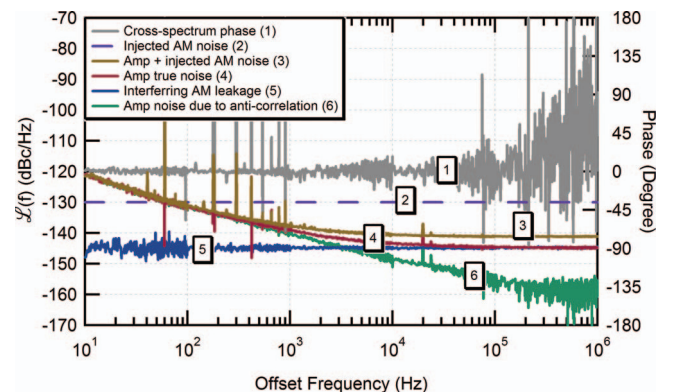


FIG. 6. Experimental results demonstrating the annihilation of DUT PM noise in a cross-spectrum measurement due to AM leakage.

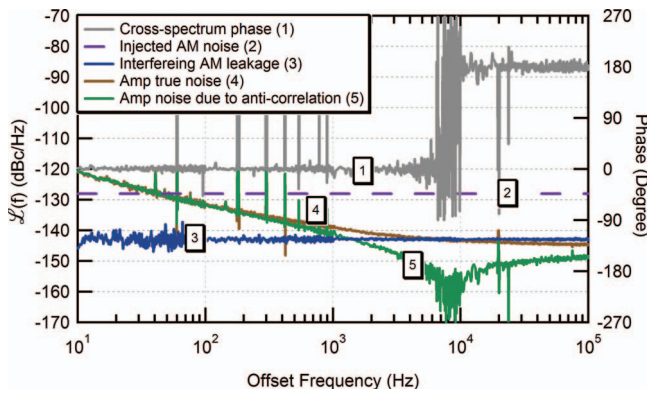


FIG. 7. Experimental results demonstrating the notch that occurs when two noise processes with different slopes intersect while one is correlated and the other is anti-correlated in the cross-spectrum.

noise of the amplifier. This causes the two noise signals to cross at an offset frequency around 10 kHz, creating a notch and grossly underestimated the noise from 300 Hz and above. The phase of the cross-spectrum in Fig. 7 clearly shows that the AM noise, dominant above 10 kHz, which is anti-correlated with a phase angle of  $\pi$ , and the PM noise, dominant below 10 kHz, have an angle of zero. In the region where the cross-spectrum is still average-limited, the phase is random.

The cancellation of noise is not limited to just AM and PM noise interactions. Any two noise sources that present themselves to both inputs of the cross-spectrum function as correlated and anti-correlated can cause this effect. A final experimental case was found where AC power line noise was coupling into the IF amplifier noise floors and interacting with an anti-correlated phase noise from the DUT. The coupled power supply noise was at a similar level as the DUT noise, producing a notch between 10 kHz and 50 kHz offset frequencies, as indicated in Fig. 8.

The correlation null has also been observed in the datasheets of commercial devices. A particular example is shown in Fig. 9 where  $f^{-1}$  AM noise leakage interacts with the  $f^{-3}$  and thermal noise corner.

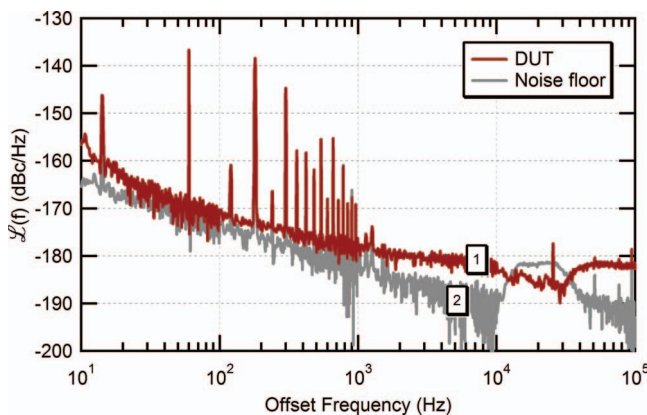


FIG. 8. Cross-spectral null observed between 10 kHz and 50 kHz offset frequencies when correlated/anti-correlated power supply noise interacts with an amplifier measurement.

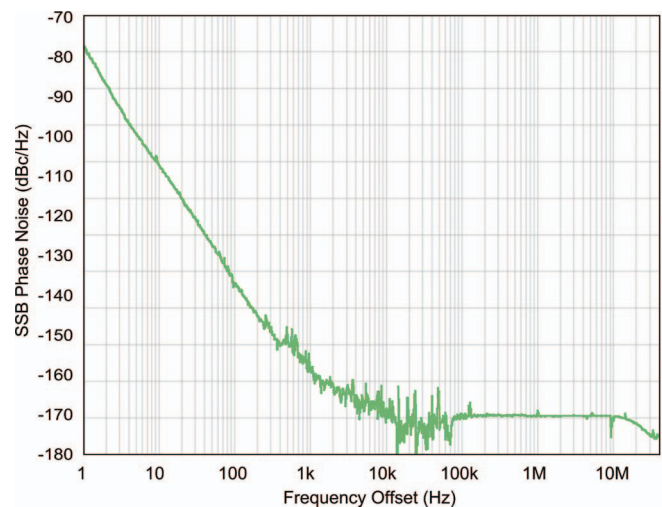


FIG. 9. Observation of a partial cross-spectral null between 3 kHz and 100 kHz. This plot is obtained from the datasheet of a commercial oscillator measured with a commercial cross-spectrum phase noise test set.

## VI. MITIGATION OF THE COLLAPSE IN CROSS-SPECTRAL PHASE NOISE MEASUREMENTS

The detection of the cross-spectral collapse after a measurement can be difficult. If an interfering signal has a phase inversion relative to the desired signal in one channel of the cross-spectrum, and has an average magnitude within  $\pm 10$  dB of the desired signal, a collapse of at least 1 dB will be observed. This can be as high as  $\sqrt{m}$  if the magnitudes are closely matched. Observing the phase of the cross-spectrum of the final measurement data can be of little help. If the measurement of the cross-spectrum is still average-limited, its phase will be random. When the interfering signal is higher than the desired signal in a region of the spectrum as in Fig. 7, a phase transition will be observed in addition to the notch in the magnitude. If the desired signal and the interfering signal have the same frequency dependent slope, it can be difficult to determine whether or not a collapse has occurred. The best method of mitigation is to analyze the interfering signals and the conversion factors prior to a measurement with the following steps:

1. Measure the AM noise of the source.
2. Adjust mixer phase shift to ensure AM leakage is sufficiently low for both mixers.

Use an AM modulator to inject an AM tone into the PM measurement and adjust the mixer quadrature point ( $\Phi$ ) for minimum leakage for both mixers. Realize that the point of minimum AM leakage is also the point of highest sensitivity; small changes in phase can lead to large changes in magnitude as well as the sign of the  $\beta$  conversion factor. Environmental and operating point changes can also affect  $\beta$ . Using a non-pure AM modulator can lead to an underestimation of the AM suppression factor and an incorrect determination of the location of “true quadrature.” A DC bias current can also be injected into the IF port of a mixer to reduce  $\beta$  or change the location of its minimum. If high levels of AM rejection are required, pure AM modulators<sup>20,21</sup> and an active servo

control of the quadrature phase shift may be a necessity. If active control is not employed, it may be beneficial to sacrifice some suppression by operating at an offset from the minimum and ensuring that changes in the sign of  $\beta$  will not occur due to operating-point fluctuations.

3. Measure the amount of AM-to-PM leakage and ensure that the AM source noise leakage is at least 10 dB below the expected PM level.
4. Ensure that both mixers are in the same operating quadrant.  
Measure the amplitude and phase conversion factors for both mixers and confirm that both mixers are operating in the same quadrant. It is important that the conversion factors for any signals presented to the cross-spectrum analyzer have the same sign in both inputs. Tuning the phase shift and observing the direction of change in the DC output voltage of the mixers can determine whether the mixer is in quadrant set (I, II) or (III, IV). Using AM and PM modulators and detecting the cross-spectral phase of the modulated tones can also determine whether the mixers are creating phase-inverted pairs or not. This can be a powerful tool for setting up a correct cross-spectral analysis.
5. Change the quadrant for one mixer so that  $\beta$  changes sign but has the same absolute value while  $k_d$  remains the same, and observe the change in the cross-spectrum. If there is a dramatic change, one of the two quadrants may be creating a collapse.
6. NEVER use a low measured noise level as an indicator for finding “true quadrature.”

The discussion in this paper focuses on the case where the desired and interfering signal are independent; however, it is also important to consider that for multiplicative, or non-thermal noise types, AM and PM noise may be correlated even if they have non-identical frequency-dependent slopes<sup>22</sup> and may cause an entirely different set of problems when cross-spectrum analysis is used.

## VII. DISCUSSION AND CONCLUSION

We demonstrate and explain a set of conditions where the detection of a desired signal in cross-spectral analysis fails partially or entirely. If two time series, each composed of the summation of two fully independent signals, are correlated in the first time signal and anti-correlated (phase inverted) in the second, and have the same average spectral magnitude, the cross-spectrum power density between two time series collapses to zero. These two conditions may occur only at localized offset frequencies or over a wide range of frequency of the cross-spectrum. The anti-correlation of one of the signals relative to the other may be caused by phase inversion, negation, time-delay, or some other mechanism. This condition initially seems counter-intuitive because the introduction of a new, independent noise signal typically does not cause a reduction of total measured noise. The simultaneous presence of correlated and anti-correlated signals can lead to gross underestimation of the total signal in cross-spectral analysis. Partial collapse of the functions still occurs when the spectral densi-

ties are close in magnitude but not equal. Cross-spectral PM noise measurements suffering from AM leakage can be particularly sensitive to these underestimations because adjustment of the mixer phase shift can easily generate correlation/anti-correlation pairs, and the level of AM leakage is widely variable and dependent on phase shift. Also, cross-spectrum analysis is commonly used in all-digital measurement systems<sup>13</sup> to reject the relatively high level of uncorrelated quantization noise in the analog-to-digital converters by 20–30 dB. This same quantization noise can also produce AM-to-PM conversion in the digital quadrature/in-phase detectors. We believe that cross-spectrum collapse may occur less frequently in digital systems because the level of AM leakage is not as prominent, and more predictable, in heterodyne digital down-converters. However, cancellation notches have still been observed in digital measurement systems after long averaging times. Finally, the photonic microwave generation from optical stabilized sources can lead to extremely low PM noise in the presence of much higher AM noise.<sup>23,24</sup> Under these conditions the probability of collapse may be high and the cross-spectrum must be evaluated and used very carefully.

## ACKNOWLEDGMENTS

The authors thank Neil Ashby, Franklyn Quinlan, Tara Fortier, Scott Diddams, Fred Walls, Enrico Rubiola, and Eugene Ivanov for theoretical and experimental discussions. We also thank Danielle Lirette, David Smith, and Mike Lombardi for help with preparation and editing this work.

<sup>1</sup>R. Vessot, L. Mueller, and J. Vanier, *Proc. IEEE* **54**, 199 (1966).

<sup>2</sup>F. L. Walls, S. R. Stein, J. E. Gray, and D. J. Glaze, in *Proceedings of the 30th Annual Symposium on Frequency Control* (IEEE, 1976), pp. 269–274.

<sup>3</sup>D. Fest, J. Gros Lambert, and J.-J. Gagnepain, *IEEE Trans. Instrum. Measur.* **32**, 447 (1983).

<sup>4</sup>G. S. Curtis, in *Proceedings of the 41st Annual Symposium on Frequency Control*, 1987 (IEEE, 1987), pp. 420–428.

<sup>5</sup>W. F. Walls, in *Proceedings of the 46th IEEE Frequency Control Symposium*, 1992 (IEEE, 1992), pp. 257–261.

<sup>6</sup>E. Rubiola and V. Giordano, *Electron. Lett.* **36**, 2073 (2000).

<sup>7</sup>E. Salik, N. Yu, L. Maleki, and E. Rubiola, in *Proceedings of the IEEE International Frequency Control Symposium and Exposition, 2004* (IEEE, 2004), pp. 303–306.

<sup>8</sup>D. Eliyahu, D. Seidel, and L. Maleki, in *Proceedings of the IEEE International Frequency Control Symposium, 2008* (IEEE, 2008), pp. 811–814.

<sup>9</sup>A. Lepek and F. L. Walls, in *Proceedings of the 1993 IEEE International Frequency Control Symposium* (IEEE, Salt Lake City, UT, USA, 1993), pp. 312–320.

<sup>10</sup>J. F. G. Nava, C. W. Nelson, and F. L. Walls, in *Proceedings of the 2000 IEEE/EIA International Frequency Control Symposium and Exhibition (Cat. No. 00CH37052)* (IEEE, Kansas City, MO, USA, 2000), pp. 506–510.

<sup>11</sup>D. A. Howe, A. Hati, C. W. Nelson, and D. Lirette, in *Proceedings of the IEEE International Frequency Control Symposium (FCS), 2012* (IEEE, 2012), pp. 1–5.

<sup>12</sup>A. Hati, C. W. Nelson, F. G. Nava, D. A. Howe, and F. L. Walls, in *Proceedings of the 2004 IEEE International Frequency Control Symposium and Exposition* (IEEE, Montreal, Canada, 2004), pp. 298–302.

<sup>13</sup>J. Grove, J. Hein, J. Retta, P. Schweiger, W. Solbrig, and S. R. Stein, in *Proceedings of the 2004 IEEE International Frequency Control Symposium and Exposition, 2004* (IEEE, 2004), pp. 287–291.

<sup>14</sup>E. N. Ivanov and F. L. Walls, in *Proceedings of the Conference on Precision Electromagnetic Measurements, Conference Digest, CPEM 2000 (Cat. No. 00CH37031)*, Sydney, NSW, Australia, 2000, pp. 447–448.

- <sup>15</sup>E. N. Ivanov and F. L. Walls, *IEEE Trans. Ultrason., Ferroelect., Freq. Contr.* **49**, 11 (2002).
- <sup>16</sup>E. Rubiola and F. Vernotte, *The Cross-spectrum Experimental Method* (2010), see <http://arxiv.org/pdf/1003.0113v1.pdf>.
- <sup>17</sup>E. Rubiola, *Phase Noise and Frequency Stability in Oscillators* (Cambridge University Press, 2010).
- <sup>18</sup>G. Cibiel, M. Regis, E. Tournier, and O. Llopis, *IEEE Trans. Ultrason. Ferroelectr. Freq. Control* **49**, 784 (2002).
- <sup>19</sup>E. Rubiola and R. Boudot, *IEEE Trans. Ultrason. Ferroelectr. Freq. Control* **54**, 926 (2007).
- <sup>20</sup>E. Rubiola, “Primary Calibration of AM and PM Noise Measurements” (2009), e-print [arXiv:0901.1073v1](https://arxiv.org/abs/0901.1073v1).
- <sup>21</sup>E. N. Ivanov, *Rev. Sci. Instrum.* **83**, 064705 (2012).
- <sup>22</sup>D. A. Howe, A. Hati, C. W. Nelson, and D. Lirette, in *Proceedings of the 2012 IEEE International Frequency Control Symposium (FCS)* (IEEE, 2012), pp. 1–5.
- <sup>23</sup>F. Quinlan, T. M. Fortier, H. Jiang, A. Hati, C. Nelson, Y. Fu, J. C. Campbell, and S. A. Diddams, *Nat. Photon* **7**, 290 (2013).
- <sup>24</sup>T. M. Fortier, F. Quinlan, A. Hati, C. Nelson, J. A. Taylor, Y. Fu, J. Campbell, and S. A. Diddams, *Opt. Lett.* **38**, 1712 (2013).